Chapter 4

Visualization and Characterization of Membrane Emulsification Using a Polycarbonate Membrane

4.1 Introduction

Cross-flow membrane emulsification has a one-step droplet formation process that a monodisperse emulsion is produced by forcing a dispersed phase through membrane pores into a continuous phase flowing across the membrane surface. This droplet formation process differs from conventional emulsification processes that an emulsion is produced by breaking up the dispersed phase fluid and/or droplets into smaller droplets in steps, which disperse in the continuous phase fluid. Membrane emulsification requires much smaller shear stress and much lower energy input than in conventional processes (Schröder *et al.*, 1998). It is important for optimization of the membrane emulsification process that we understand how droplets grow and detach from the membrane pores. Peng and Williams (1998) used a high-speed video camera to observe the droplet formation process from a single circular capillary as a membrane pore model. They also analyzed the influence of the process parameters, such as the continuous-phase flow velocity and the dispersed phase pressure, on the droplet growth and detachment processes.

We recently developed a micro-visualization system of membrane emulsification composed of a novel membrane module and a microscope video system (Kukuchi *et al.*, 1992). This system enables one to observe the droplet formation process from a porous membrane and to analyze interaction between adjacent droplets growing on a porous membrane, which provides a significant influence on the droplet formation behavior. In the present chapter, we discussed the results of direct observations of oil droplet formation at the surface of a hydrophilic polycarbonate membrane with cylindrical pores during cross-flow membrane emulsification. The influences of some of the fundamental process parameters such as the continuous-phase flow velocity and the surfactant type on the membrane emulsification were also investigated.

4.2 Materials and Methods

Materials

Soybean oil (Wako Pure Chemical Ind., Osaka, Japan) was used as the dispersed

phase. MilliQ water (Millipore Co., Massachusetts, USA) was used to prepare all of the continuous phase solutions. The surfactants used in this chapter were sodium dodecyl sulfate [SDS], polyoxyethelene (20) sorbitan monolaurate [Tween20; hydrophilic lipophilic balance (HLB), 13], tri-n-octyl-methylammonium chloride [TOMAC] (Wako Pure Chemical Ind., Osaka, Japan), and pentaglycerol monolaurate [PGM, >65% purity; Sun soft A-121E; HLB, 12] (Taiyo Kagaku Co. Ltd., Mie, Japan). We applied a surfactant concentration over the critical micelle concentration (CMC), determined by the interfacial tension measurement (Tong *et al.*, 2000), to assure the sufficient supply of a surfactant at the interface.

Experimental setup

A disk-type hydrophilic polycarbonate membrane with 10 μm-mean pore size and 10 μm-thick (ISOPORE^{TM}, Nihon Millipore Co., Tokyo, Japan) was employed in this chapter. The scanning electron microscopy (SEM) photograph in Fig. 4.1 indicates that the polycarbonate membrane possesses uniformly sized cylindrical pores. The membrane emulsification system, schematically depicted in Fig. 4.2, consists of a membrane module, a reservoir or a syringe pump to feed the dispersed phase, a peristaltic pump to feed the continuous phase, and the microscope video system. Detailed information about the microscope video system can be found in previous papers (Kikuchi *et al.*, 1992; Kawakatsu *et al.*, 1997). A 24-mm square of polycarbonate membrane, with two feed-holes for the dispersed phase penetrated at the corners of the membrane, was mounted between two rubber spacers in the membrane module. The membrane, set in the module, has a measured effective membrane area of 1.46 cm^2. The thickness of continuous phase fluid film above the membrane surface is approximately 500 μm. The membrane emulsification behavior was observed with total magnifications of 500 to 2000 through an optically flat acryl plate, a metallographic microscope (MD-300EF, Nikon Co., Tokyo, Japan) and a charge coupled device (CCD) color camera (KP-C550, Hitachi, Tokyo, Japan), and was recorded with a video recorder (EV-PR2, Sony Co., Tokyo, Japan).
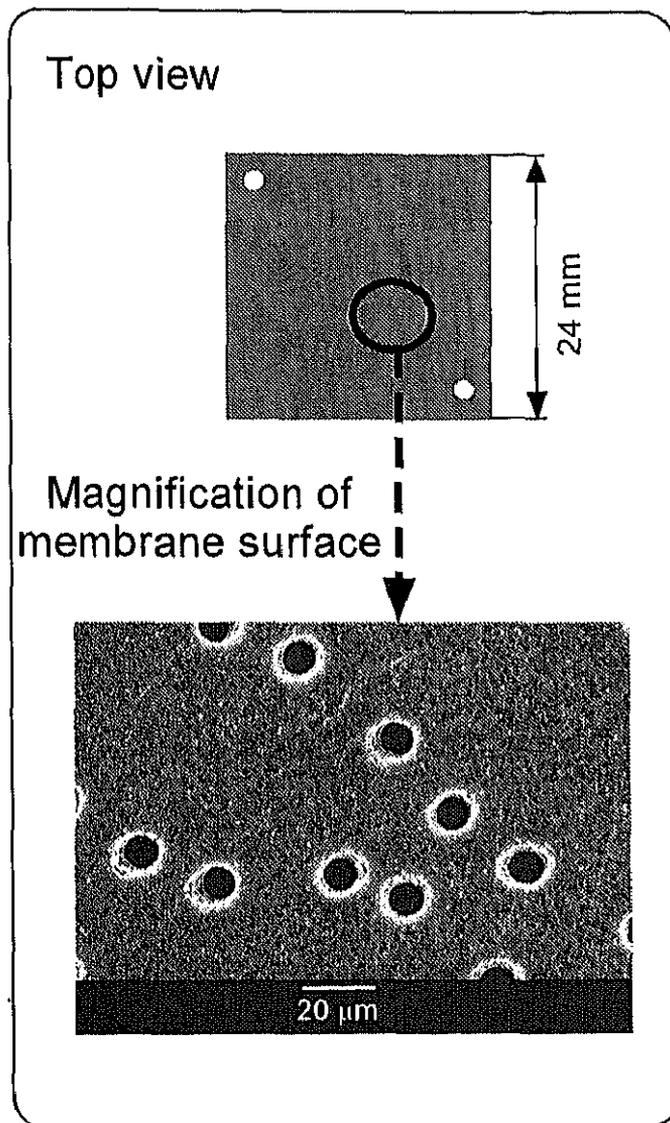
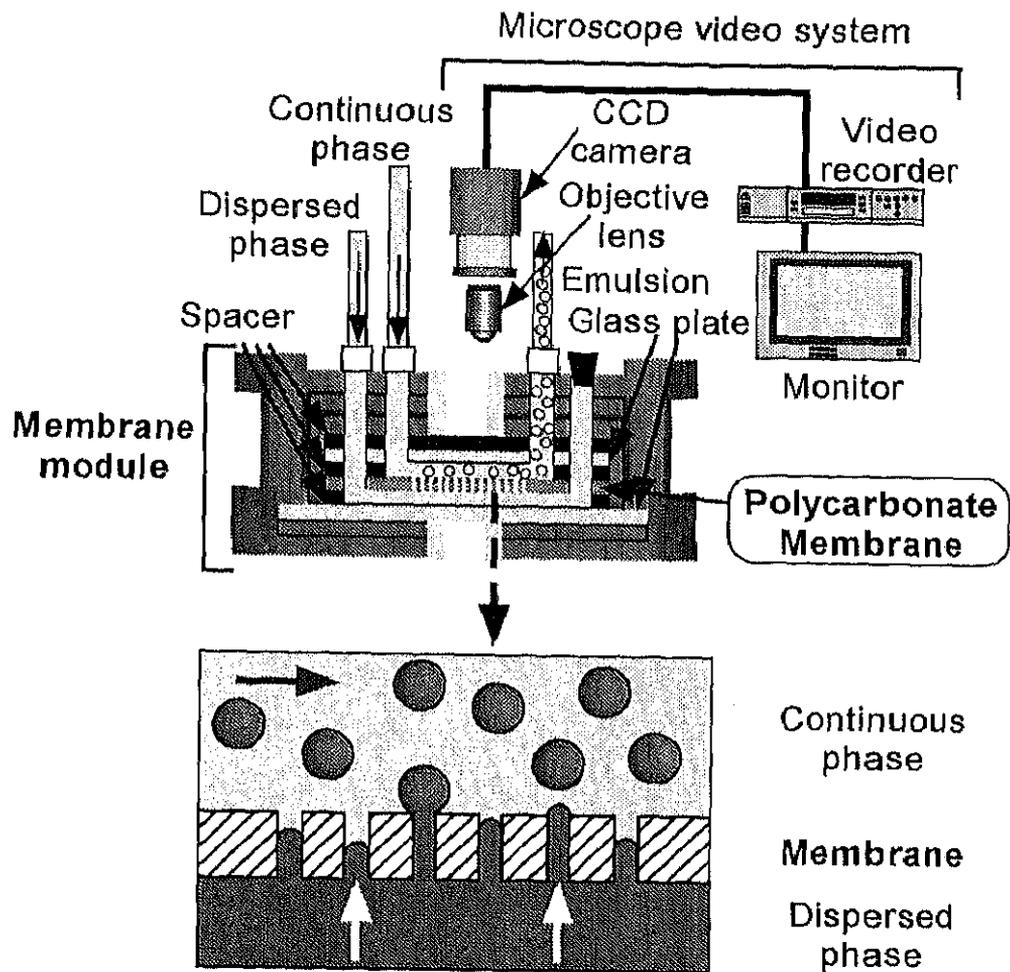Fig. 4.1 Schematic and SEM photograph of polycarbonate membrane used in this chapter.

Fig. 4.2 Experimental setup for cross-flow membrane emulsification.

Membrane emulsification

Microscopic observation of membrane emulsification: Soybean oil was used as the dispersed phase, and 0.3 wt.% SDS aqueous solution was used as the continuous phase. A polycarbonate membrane presoaked in the continuous phase liquid was mounted in the module filled with the continuous phase. A peristaltic pump (AP-2250, Advantec Toyo Co., Tokyo, Japan) was employed to feed and recover the continuous phase with its flow velocity of 0.023 m/s. The dispersed phase, pressurized in steps by raising the reservoir, was achieved on the bottom side of the membrane via the flow path for the dispersed phase. At an applied pressure exceeding the breakthrough pressure, the dispersed phase broke through the membrane, and then commenced droplet formation (Fig. 4.2). The oil droplets formed were recovered by the regulated continuous-phase flow.

Influence of the process parameters: The surfactants used in this chapter were added to either the continuous phase or the dispersed phase at a given concentration over CMC (described in a later section). A peristaltic pump (505U, Watson-Marlow Ltd., Cornwall, UK) was used to feed the continuous phase. This pump enables a maximum flow velocity of 0.63 m/s in the module utilized in this chapter. We also used a syringe pump (Model 11, Harvard Apparatus Inc., Massachusetts, USA) to feed the dispersed phase, with flow rates through the membrane of 15-20 ml/h (oil permeate flux of 102-137 $l/(m^2 \ h)$). All the other emulsification processes and conditions were the same as described in the above section.

Measurements and analysis

The droplet formation behavior from a polycarbonate membrane was analyzed from the video images recorded with the microscope video system. The average droplet diameter and coefficient of variation of the prepared emulsions were determined by counting over 200 droplets on image processing software (WinRoof, Mitani Co., Fukui, Japan) after capturing the droplet images on a personal computer. The coefficient of

variation, of which definition was described in Chapter 2.2, was used to present the droplet size distribution.

The interfacial tension measurement method was described in Chapter 2.2. The contact angle between an oil droplet and the membrane surface in the continuous phase was also measured from the photograph of an oil droplet in contact with the membrane surface.

4.3 Results and Discussion

Microscopic observation of membrane emulsification

Figure 4.3 illustrates the typical behavior of oil droplet formation from a polycarbonate membrane. The dispersed phase, pressurized at a breakthrough pressure of 1.35 kPa, passed through the pores and began to grow as a droplet at the pore tip (Figs. 4-3a and b). The almost spherically shaped droplet continued growing while swinging at the pore tip, depending on the fluctuating continuous phase flow (Figs. 4.3b-e). When the droplet diamater in this case reached about 65 μm, the droplet detached from the pore tip (Fig. 4.3f), and an O/W emulsion droplet was formed (Fig. 4.3g). Droplet growth from the pore tip then commenced again. This repeated droplet formation process led to the preparation of an O/W emulsion. The polycarbonate membrane yielded almost uniformly sized droplets from each pore, whereas the droplet size depended on the site of the pores. This indicates less monodispersity of the prepared O/W emulsion. Approximately 1% of the pores formed droplets in this case (Fig. 4.3a), and the larger pores began to preferentially form droplets. The droplet formation rate per pore was estimated as follows. A polycarbonate membrane used in this chapter has about 6×10^4 pores/cm^2, indicating 600 pores/cm^2 form oil droplets with a pore efficiency of 1%. From the experimental conditions, the droplet formation rate was estimated to be about 1 droplet/s. The droplet formation rates per pore measured by microscopic observations supported the estimated value. It should be mentioned that the droplet formation rate depended on the site of the pores because of the significant pressure gradient on the micron
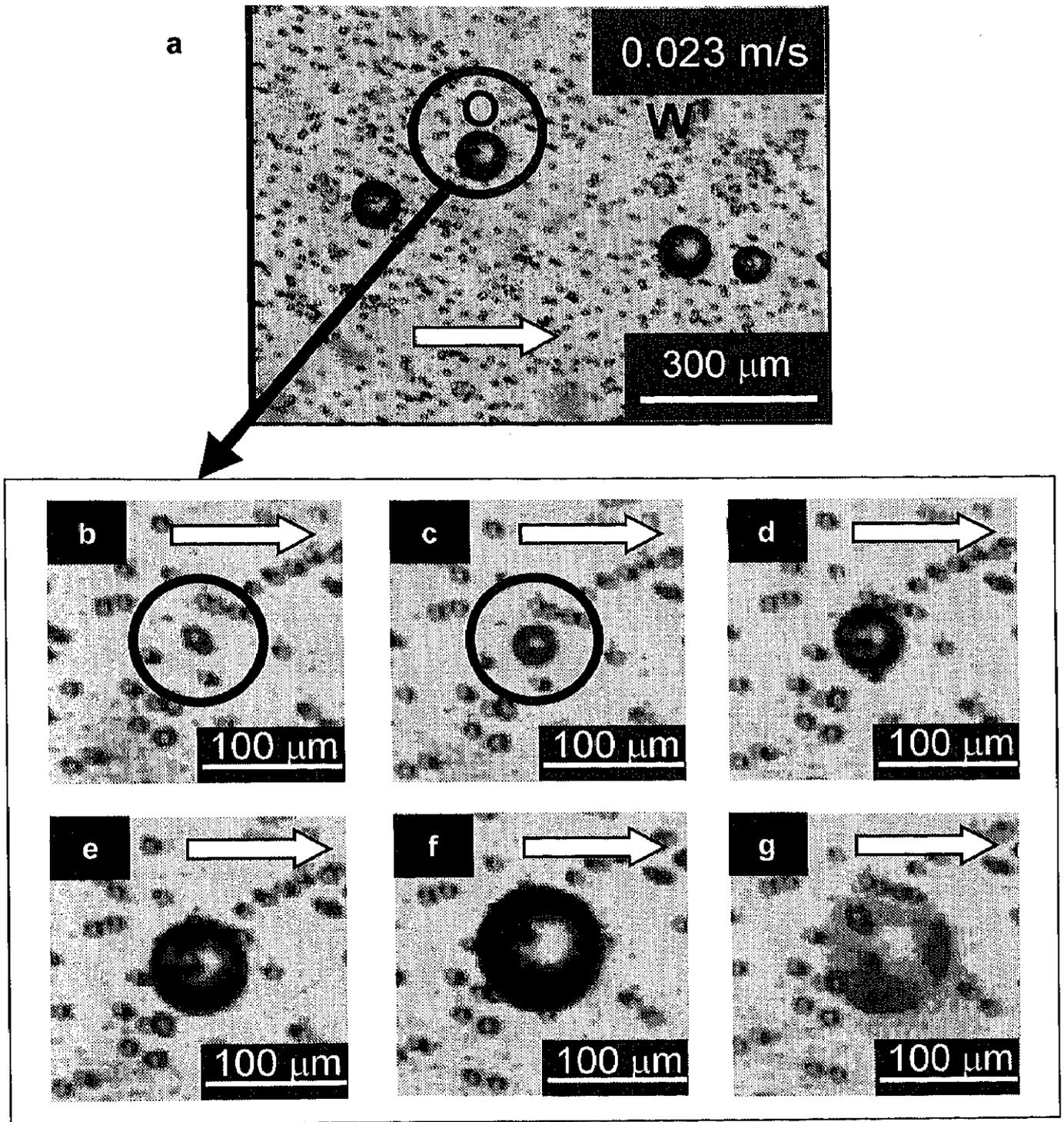
58

Fig. 4.3 Microscopic photographs of the membrane emulsification process for soybean oil / water (0.3 wt.% SDS) system. (a) Droplet formation from the polycarbonate membrane; (b)-(g) sequence of the droplet formation from a membrane pore.

scale.

Some studies on membrane emulsification (Schröder and Schubert, 1999; Peng and Williams, 1998) suggest that the drag force due to the continuous phase flow may cause shearing of growing droplets and their detachment from the pore tip. We also conducted polycarbonate membrane emulsification without the continuous phase flow to visually determine whether the continuous phase flow actually works as the driving force to form emulsion droplets. Although droplet growth up to the clearance in the module (approximately 500 μm) was observed from some pores, little droplets detached from the pore tip during the experimental runs. This result verifies that shear force from the continuous phase flow was required to make emulsion droplets detach from the pore tip in this membrane emulsification.

The membrane emulsification system with a micro-visualization system enabled the microscopic observations of the membrane emulsification process and helped us analyze the droplet formation behavior. Therefore, the fundamental characteristics of O/W polycarbonate membrane emulsification were further investigated by utilizing the membrane emulsification system.

Influence of the continuous-phase flow velocity

The continuous-phase flow velocity is one of the fundamental process parameters that determine the membrane emulsification characteristics. The influence of the continuous phase flow velocity on the membrane emulsification was first investigated. A 0.3 wt.% SDS aqueous solution was used as the continuous phase. The average flow velocity was varied from 0.023 to 0.54 m/s under a fixed dispersed phase flux of 137 l/(m^2 h). Figure 4.4 shows the influence of the continuous-phase flow velocity on the average droplet diameter. The average droplet diameters of the prepared O/W emulsions decreased significantly with an increase in the flow velocity range in below 0.3 m/s. When the flow velocity exceeded 0.3 m/s, the average droplet diameters of the prepared emulsions remained almost constant at about 20 μm. The microscopic photographs of the
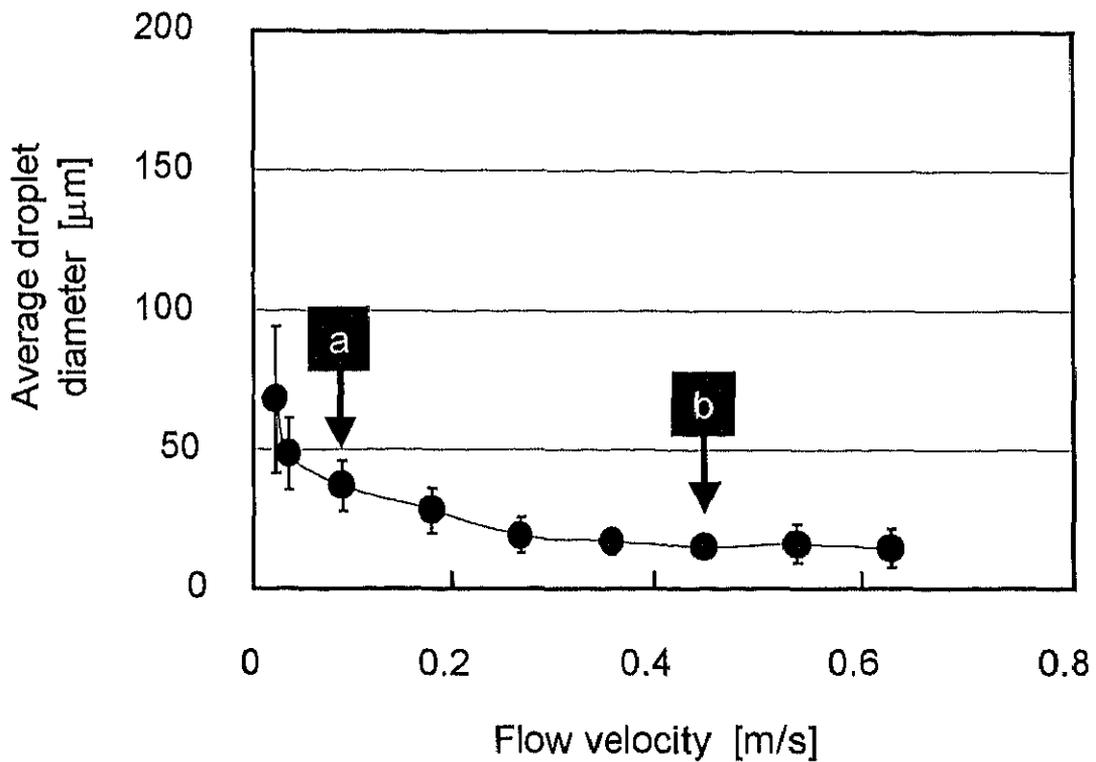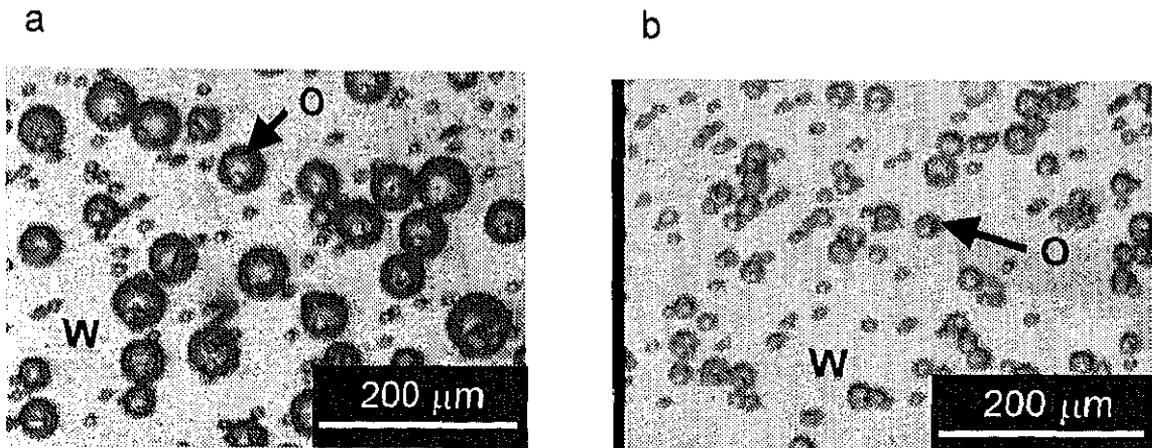
Fig. 4.4 Influence of the continuous-phase flow velocity on the average droplet diameter for a soybean oil / water (0.3 wt.% SDS) system. (a), (b) Microscopic photographs of the membrane emulsification process.

membrane emulsification process in Figs. 4.4a and b also exhibited a change in the size of the growing droplets. The coefficients of variation of the prepared emulsions were between 20 and 50%, which showed less monodispersity than the minimum coefficients of variation of approximately 10% in membrane emulsification (Omi et al., 1994). The droplet shape during the droplet growth process tended to become distorted at high flow velocities (Fig. 4.4b). We also observed that some adjacent droplets growing on the membrane surface were in contact, particularly at flow velocities lower than 0.1 m/s. This causes droplet detachment before they have undergone sufficient growth to be sheared by the continuous phase flow, resulting in broader droplet size distributions. However, no droplet coalescence occurred during the droplet formation process. As a result, high flow velocities were found to yield stable membrane emulsification.

The influence of the continuous-phase flow velocity on the droplet size and size distribution has been discussed here. The change in the average droplet diameters of the emulsions prepared by membrane emulsification exhibited a similar tendency to that using porous glass and ceramic membranes (Schröder and Schubert, 1999; Joscelyne and Trägårdh, 1999; Katoh et al., 1996). This tendency can be explained by the types and balance of the forces acting on a droplet growing through a pore. The external forces acting on the droplet are described in detail elsewhere (Peng and Williams, 1999; Schröder et al., 1998). To make droplets detach from the pore tip, the shear force due to the continuous phase flow that induces the droplet detachment must exceed the interfacial tension force that restricts it. An increase in the flow velocity yields a stronger shear force that can balance the interfacial tension force at a smaller droplet size. We considered that this leads to the decrease in the resultant droplet size with increases in the flow velocity. Microscopic observations of the membrane emulsification process in this chapter also proved that the above-mentioned theory was valid. The coefficients of variation of the O/W emulsions prepared using a polycarbonate membrane depended only minimally on the flow velocity. There was little droplet coalescence before droplet detachment, even at low flow velocities applied in this chapter. Porous membranes with

short pore intervals may cause droplet coalescence on the membrane surface at low flow velocities, which results in broader droplet size distributions (Schröder and Schubert, 1999; Joscelyne and Trägårdh, 1999; Katoh et al., 1996). The low porosity of the polycarbonate membrane and the rapidly adsorbing surfactant (SDS) used would prevent coalescence between adjacent droplets. Little droplet coalescence over the applied flow velocities may have led to insignificant influence of the flow velocity on the coefficients of variation of the prepared emulsions.

Influence of surfactant type

Membrane emulsification using anionic, nonionic, and cationic surfactants: The type of surfactant also plays a critical role in the membrane emulsification behavior. The surfactant influence on the membrane emulsification was investigated using different surfactants. We first used SDS as an anionic surfactant, dissolving it into the continuous phase at a concentration of 0.3 wt.%. Table 4.1 shows the experimental conditions, measured contact angles, and interfacial tensions. In this case, the stable droplet formation without droplet coalescence was carried out over the applied flow velocities (Figs. 4.4 a and b). The emulsification characteristics using SDS as the surfactant were described in detail before in this section. The results in this chapter demonstrate that SDS is appropriate for stable preparation of O/W emulsions using a polycarbonate membrane.

Polycarbonate membrane emulsification using nonionic surfactants was next performed. Nonionic surfactants are of great significance in preparing food and pharmaceutical emulsions (McClements, 1999; MartiWestres and Nielloud, 2000). Two nonionic surfactants, PGM and Tween20, were used considering the various conditions necessary for stable preparation of O/W emulsions. Each surfactant was dissolved in the continuous phase at a concentration of 1.0 wt.%. The dispersed phase flux was regulated at 102 l/(m^2 h). The influence of the flow velocity on the average droplet diameter is shown in Fig. 4.5b for PGM and in Fig. 4.6b for Tween20. The average droplet diameters of the prepared O/W emulsions for both nonionic surfactants decreased as the

Table 4.1 Contact angle and interfacial tension of the experimental systems used.

Surfactant[a]	Condition	Contact angle[b] (deg)	Interfacial tension (mN/m)
SDS	0.3 wt% (W)[c]	106	4.0
PGFE	1.0 wt% (W)	102	4.4
Tween20	1.0 wt% (W)	95.2	2.5
TOMAC	2.0 wt% (O) [d]	26.6	3.1

[a]SDS, sodium dodecyl sulfate; PGM, polyglycerol monolaurate ; Tween20, polyoxyetylene (20) sorbitan monolaurate; TOMAC, tri-n-octylmethylammonium chloride.
[b]Contact angle between an oil droplet and the membrame surface in the water phase.
[c]Dissolved in the continuous water phase.
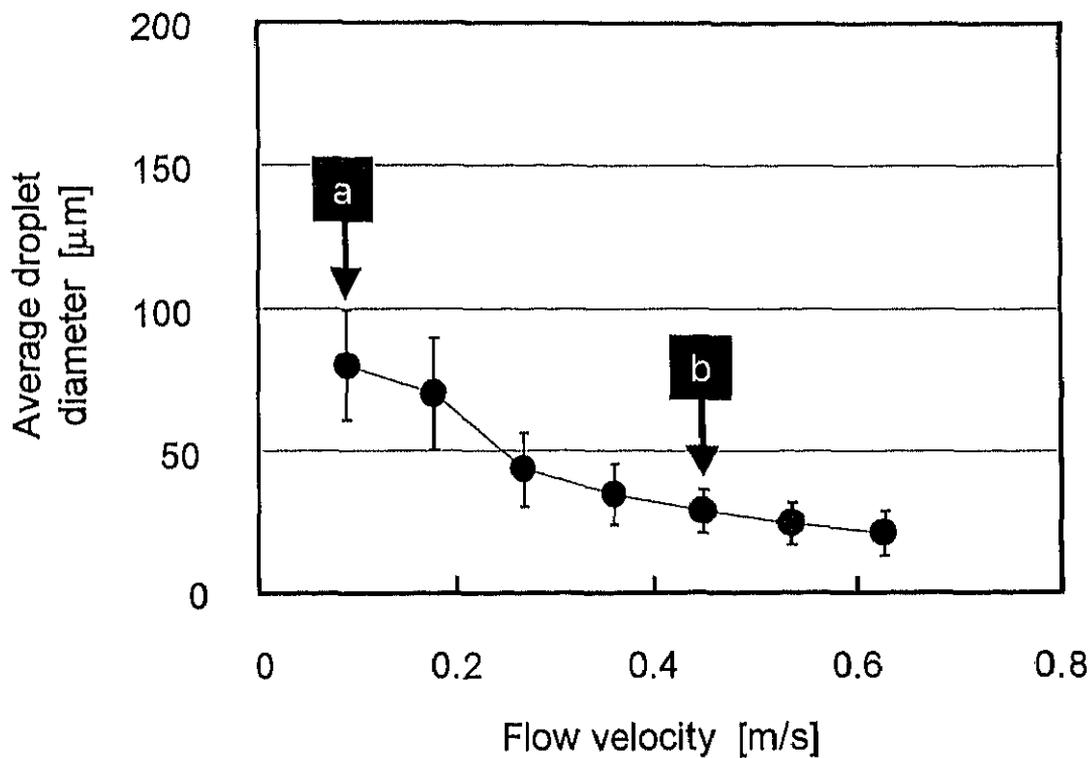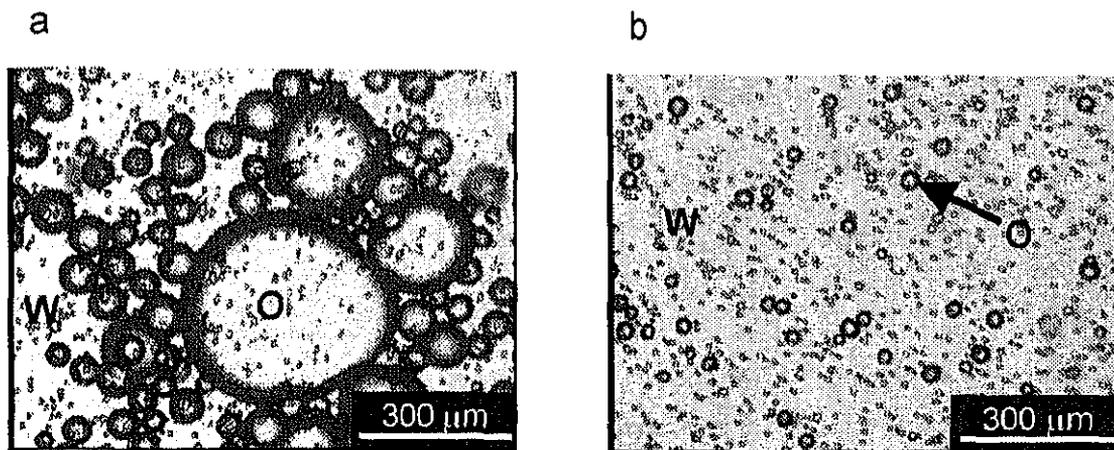[d]Dissolved in the dispersed oil phase.

Fig. 4.5 Influence of the continuous-phase flow velocity on the average droplet diameter for a soybean oil / water (1.0 wt.% PGM) system. (a), (b) Microscopic photographs of the membrane emulsification process.
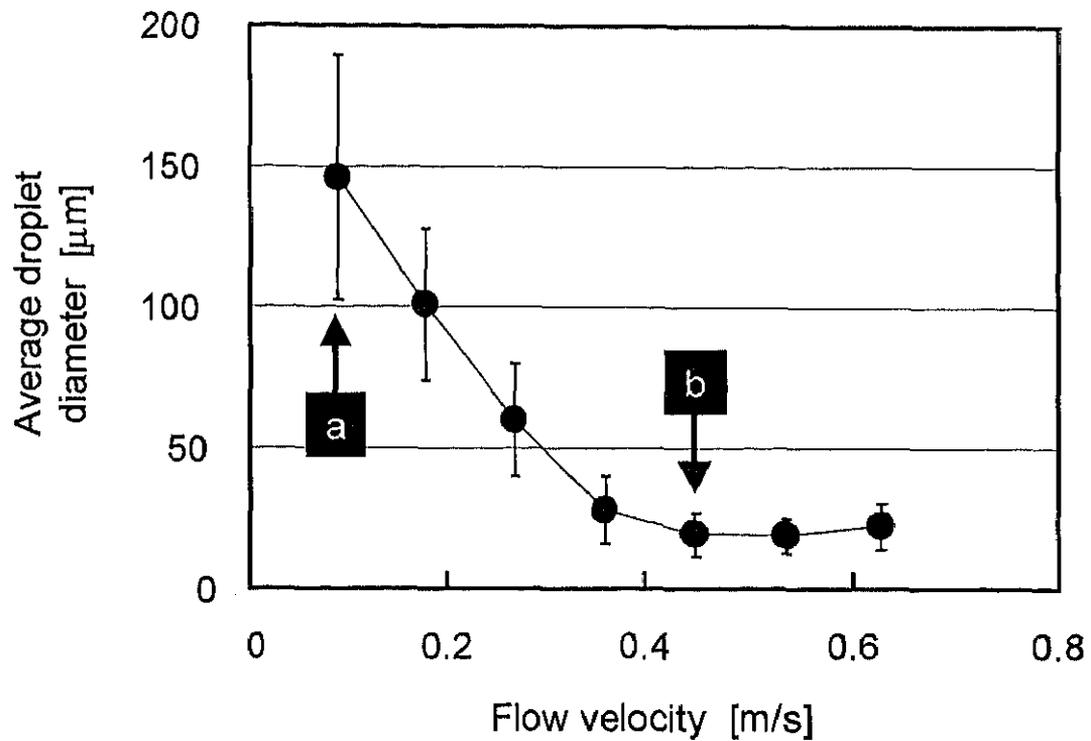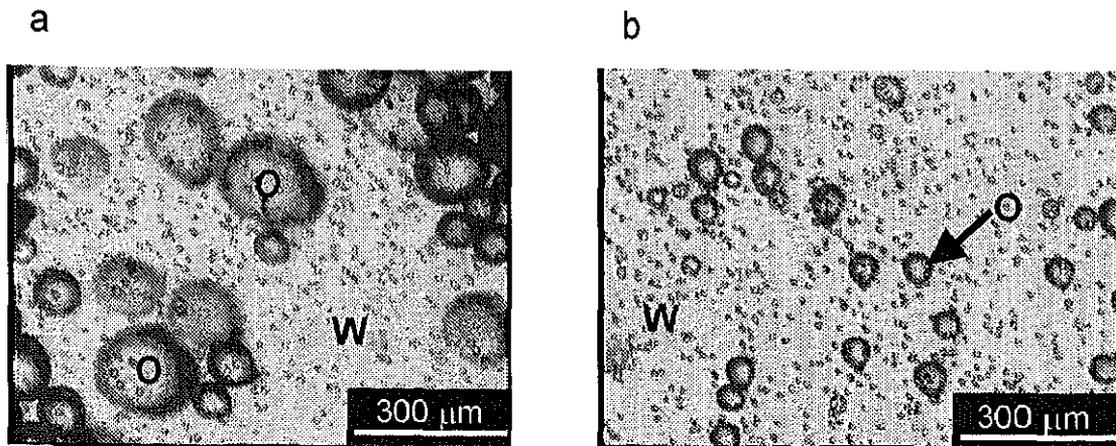
Fig. 4.6 Influence of the continuous-phase flow velocity on the average droplet diameter for a soybean oil / water (1.0 wt.% Tween20) system. (a), (b) Microscopic photographs of the membrane emulsification process.

flow velocity increased, becoming almost constant at flow velocities greater than 0.4 m/s. The average droplet diameters for PGM and Tween20 were slightly larger than those for SDS over the applied flow velocities. Additionally, the Tween20-containing system tended to yield larger droplets than the other systems employed, especially at flow velocities lower than 0.3 m/s. The coefficients of variation of the emulsions prepared using nonionic surfactants ranged from 25 to 40% for PGM and 25 to 45% for Tween20. The microscopic photographs in Figs. 4.5a and 6a illustrate that successful membrane emulsification was carried out at the flow velocities higher than 0.1 m/s. However, in addition to the droplet formation from the membrane pore, these nonionic surfactant-containing systems caused droplet wetting on the membrane at flow velocities lower than 0.1 m/s. The preceded results revealed that the nonionic surfactants used have superior ability for membrane emulsification in flow velocity ranges greater than 0.1 m/s.

Polycarbonate membrane emulsification was also conducted using a cationic surfactant (TOMAC), dissolved in the dispersed phase at a concentration of 2.0 wt.%. Figure 4.7 depicts the membrane emulsification process using TOMAC as the surfactant. The dispersed phase that broke through some membrane pores spread smoothly on the membrane surface and completely replaced the continuous phase. No droplet formation was observed during the experimental runs, which is similar to the microchannel emulsification behavior using TOMAC (Tong et al., 2000). The wetting properties of an oil droplet on the membrane surface can be explained by the surfactant-membrane surface interaction and the measured contact angle (see below in this section). As a result, there was a difficulty in preparing O/W emulsions using the polycarbonate membrane with the cationic surfactant.

Analysis of membrane emulsification behavior: Maintaining the hydrophilicity of the membrane surface is a prerequisite for stable preparation of emulsions by membrane emulsification (Nakashima et al., 1991; Katoh et al., 1996) and MC emulsification (Tong et al., 2000). The surfactant-membrane surface interaction is a key factor that affects the
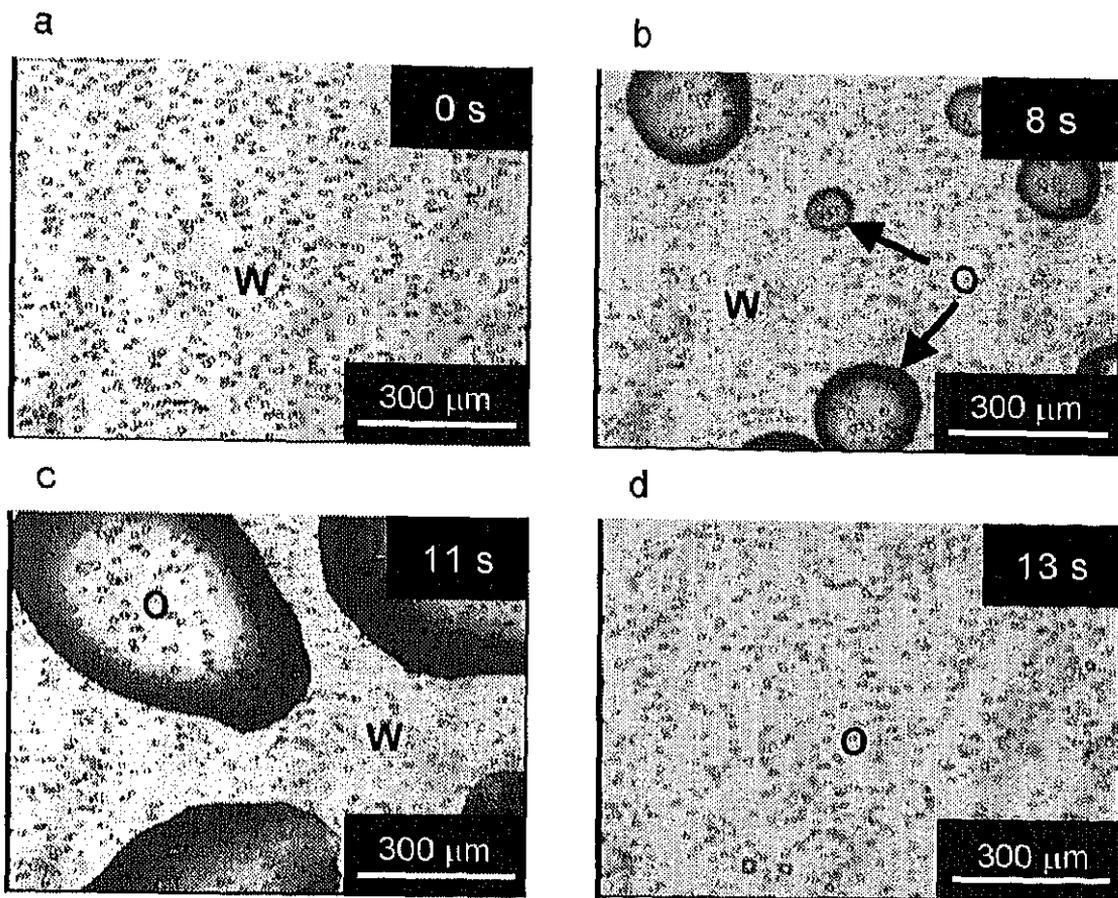
Fig. 4.7 Microscopic photographs of wetting of the dispersed oil phase on a membrane surface for a soybean oil (2.0 wt.% TOMAC) / water system.

hydrophilicity of the membrane surface. The contact angle is also a useful parameter for understanding the wetting properties of the membrane surface by the dispersed phase. The measured contact angle data for the experimental systems with the different surfactants used are shown in Table 4.1. The electric repulsive interaction works between the negatively charged group of SDS and the membrane surface with negative zeta potential (Bowen and Cooke, 1991; Lettmann et al., 1999) for the case of an anionic surfactant (SDS), keeping the membrane surface hydrophilic during the membrane emulsification process. The measured contact angle of 106° for the SDS-containing system supported this idea. Moreover, this rapidly adsorbing SDS has the advantage of preventing droplet coalescence during droplet formation. Hence, we considered that this SDS-containing system had the potential to perform stable membrane emulsification. Nonionic surfactants have no strong repulsion with the membrane surface, which differs from anionic surfactants. The measured contact angles of 102° and 95.2° for PGM- and Tween20-containing systems were slightly lower than that for the SDS-containing system. This suggests that the membrane surface can remain hydrophilic during membrane emulsification. However, these systems performed unstable membrane emulsification at low flow velocities (Figs. 4.5a and 4.6a). The slow adsorption of these nonionic surfactants at an interface would cause droplet coalescence on the membrane surface, which results in wetting of the dispersed phase on the membrane surface. On the other hand, a positively charged TOMAC easily adsorbs on the membrane surface because of the strong affinity with the negatively charged membrane surface. The low contact angle of 26.6° for the TOMAC-containing system also indicates complete wetting of the dispersed phase on the membrane surface; therefore, a dispersed phase with TOMAC would have spread without any droplet formation on the membrane surface.

The resultant droplet diameters for the PGM- and Tween20-containing systems tended to become larger than those for the SDS-containing system over the applied flow velocities. These three experimental systems have similar interfacial tensions, as shown in Table 4-1.

Nevertheless, there is a difference in the adsorption kinetics of the surfactants at an interface. Schröder *et al.* (1998) reported that SDS adsorbed more rapidly at an oil/water interface than Tween20, and that the rapidly adsorbing SDS promotes droplet detachment at a smaller droplet diameter. PGM is also a slowly adsorbing surfactant compared to SDS. It is therefore assumed that slow adsorption of PGM and Tween20 at the interface was the primary reason for the formation of larger droplets from the polycarbonate membrane.

4.4 Conclusions

In the present chapter, we have verified the continuous phase flow-driven droplet formation from cylindrical membrane pores through microscopic observations of O/W polycarbonate membrane emulsification. This indicates that the continuous phase flow is a predominant parameter for determining the resultant droplet diameter. The influence of the flow velocity on the average droplet diameters of the prepared emulsions became less significant at high flow velocities greater than 0.4 m/s, and the resultant emulsions had the average droplet diameters of about 20 μm and the coefficients of variation of 20 to 50%. The anionic and nonionic surfactants used in this chapter were suitable for performing successful O/W membrane emulsification. The repulsive surfactant-membrane surface interaction prevented adsorption of these surfactants on the negatively charged membrane surface, contributing to maintaining the hydrophilicity of the membrane surface, which is a prerequisite for stable membrane emulsification. Nevertheless, the slowly adsorbing nonionic surfactants resulted in unstable droplet formation at low flow velocities less than 0.1 m/s. When a cationic surfactant-containing system was employed, the dispersed phase that broke through the membrane pores immediately spread and wetted on the membrane surface due to the strong surfactant-membrane surface affinity. Thus, microscopic observations of the membrane emulsification process enabled a better understanding of the characteristics of the droplet formation from the membrane pores and the influence of the process parameters, such as the continuous phase flow and the

surfactant type.